

# Gapped Low Energy Excitations Across an Entanglement Percolation Transition in the Quantum Spin Liquid Candidate NaYbSe<sub>2</sub>

Luke Pritchard Cairns,<sup>1,\*</sup> Yuanqi Lyu,<sup>1,†</sup> Chunxiao Liu,<sup>1</sup> Josue Rodriguez,<sup>1,2</sup> Kenneth Ng,<sup>1</sup> John Singleton,<sup>3</sup> and James G. Analytis<sup>1,2,4,5,‡</sup>

<sup>1</sup>*Department of Physics, University of California, Berkeley, California 94720, USA*

<sup>2</sup>*Materials Science Division, Lawrence Berkeley National Laboratory, Berkeley, California 94720, USA*

<sup>3</sup>*National High Magnetic Field Laboratory, Los Alamos National Laboratory, Los Alamos, New Mexico 87545, USA*

<sup>4</sup>*CIFAR Quantum Materials, CIFAR, Toronto, Canada*

<sup>5</sup>*Kavli Energy NanoScience Institute, Berkeley, CA, USA*

(Dated: July 8, 2024)

The study of quantum magnetism in frustrated triangular lattices has promised the discovery of exotic excitations emerging from many-body entanglement, like the quantum spin liquid. This field is vexed by the interplay of disorder, correlations and long-range order, whose properties are challenging to control and disentangle. We study the entropy-carrying excitations of a leading candidate in this search, the material NaYbSe<sub>2</sub>, as a function of site dilution to directly address this challenge. We map the evolution of the entangled spins across the percolation transition, showing unequivocal evidence for the presence of an energy gap in the excitations of the system. However, we also show that this gap onsets at the percolation transition where disorder is the greatest, strongly suggesting that it is unlikely to be associated with a quantum spin liquid. Instead we suggest the more universal scenario of a short-range ordered state with entropy-carrying boundaries.

## INTRODUCTION

The quantum spin liquid (QSL) is a ground state in which magnetic interactions lead to many-body entanglement but no long-range order. It is the subject of intense study due to the exotic nature of its excitations, its connection to the problem of high- $T_c$  superconductivity, and its potential application in the field of topological quantum computing. Geometric frustration generally plays a key role in the suppression of long-range order, and experimental realisations of the triangular magnetic lattice are thus highly sought after. It is now well established that antiferromagnetic Heisenberg interactions on the triangular lattice lead to long-range ordering at zero-temperature [1], but this ordering can be suppressed with the addition of appropriately tuned anisotropic exchange terms or next-nearest neighbour interactions [2, 3]. In this narrow region of parameter space a QSL ground state is predicted to emerge, although the exact nature—and by extension whether the low-energy excitations might be gapped—is still under debate [4–7].

The experimental situation is often muddled by the presence of disorder and glassy dynamics, where the interplay of correlation length and scattering length complicates a clear identification of the underlying physics. The hunt for a clean physical manifestation of the QSL has motivated intense study into the class of delafossite compounds AYbSe<sub>2</sub> (where A is an alkaline metal) [8–10]. In these materials, magnetic Yb<sup>3+</sup> ions form layers of well separated two-dimensional triangular lattices, and the crystal field split pseudospin- $\frac{1}{2}$  moments can naturally give rise to interaction terms beyond Heisenberg exchange. Although recent studies have shown that both CsYbSe<sub>2</sub> and KYbSe<sub>2</sub> do exhibit 120° order [11, 12],

the strength of the next-nearest neighbour interaction appears to scale inversely with the size of the alkaline metal atomic radius. A continuation of this trend would place NaYbSe<sub>2</sub> inside—or near to—the region of parameter space wherein the magnetic order is suppressed completely (note, LiYbSe<sub>2</sub> unfortunately crystallises in a different structure [13]). Indeed, no measurements thus far have detected any long-range order in NaYbSe<sub>2</sub> down to 40 mK.

However, the verification of a QSL ground state in NaYbSe<sub>2</sub> is immensely challenging. This is fundamentally because the properties of the ground state can only be inferred through observable low-energy excitations at finite temperatures. Further, signatures of the QSL ground state can be mimicked by defects and inhomogeneities, or simply by classical physics [14, 15]. As an example to illustrate this problem, inelastic neutron scattering data on NaYbSe<sub>2</sub> have been interpreted as evidence for a spinon Fermi surface [16], whereas the emergence of magnetic order in the closely related compound KYbSe<sub>2</sub> led the authors to suggest that NaYbSe<sub>2</sub> must instead host a gapped  $\mathbb{Z}_2$  spin liquid [12]. Clearly then, in order to consolidate and understand the growing abundance of experimental findings, novel approaches are necessary.

In this work, through low-temperature thermodynamic measurements of the compositional series NaYb <sub>$x$</sub> Lu <sub>$1-x$</sub> Se<sub>2</sub>—comprised of homogeneous mixtures of magnetic Yb<sup>3+</sup> and nonmagnetic Lu<sup>3+</sup> [17]—we track the evolution of the entropy-carrying excitations across the percolation transition of the many-body magnetic lattice. The introduction of non-magnetic sites breaks the triangular lattice into smaller magnetic clusters, such that the parameter  $x$  can be used to tune the connectiv-

ity, fractional dimension and the related geometric frustration of the magnetic  $\text{Yb}^{3+}$  lattice. This allows for a distinction between excitations emerging from large-scale entanglement versus those which only require a percolation of magnetic sites, or arising from smaller disconnected magnetic clusters.

We find direct evidence for gapped magnetic excitations in  $\text{NaYbSe}_2$ , a crucial finding that at first sight is consistent with the existence of a  $\mathbb{Z}_2$  QSL with topological excitations. However, this gapped excitation emerges sharply near the percolation threshold ( $x = 0.5$  for the triangular lattice), implying that frustration is not necessary in its formation. With proximity to magnetic order the gap feature is suppressed and inside the antiferromagnetic state the magnetic thermal conductivity is instead well explained by a magnon heat current. We give an alternative interpretation of our data, invoking networks of one-dimensional boundaries of a short-range ordered system. We suggest that this picture might be ubiquitous, and explain similar behaviour observed in many candidate QSL materials.

## RESULTS

Detailed descriptions of the crystal growth, characterisation and evidence for homogeneity of magnetic and non-magnetic sites in the  $x < 1$  compounds can be found in [17]. Heat capacity measurements were performed using a Quantum Design PPMS Dynacool with  $^3\text{He}$  insert for  $T > 1\text{ K}$  and a home-built dilution refrigerator setup for  $T < 1\text{ K}$ . The data was acquired using the relaxation time method [18] across the full temperature range, and analysed in the low-temperature region using a modified version of the full temperature response analysis described in [19]. Thermal conductivity measurements were also performed using a home-built dilution refrigerator setup, using a standard steady-state one heater, two thermometers method. All measurements were performed on single crystals.

### Excitations in the Disordered State

Shown in FIG. 1 (a) is the zero-field heat capacity of the compositional series  $\text{NaYb}_x\text{Lu}_{1-x}\text{Se}_2$ . In the compound with only 5% of magnetic sites the heat capacity peak is almost entirely attributable to the condensation of dimers into singlets. The position of the peak thus defines the energy scale of interaction, and the data is fit well by a Heisenberg model with  $J/k_B = 6.1\text{ K}$  (included in the supplementary material (SM) are more sophisticated attempts to constrain the pseudospin- $\frac{1}{2}$  Hamiltonian through models of  $\text{NaYb}_{0.05}\text{Lu}_{0.95}\text{Se}_2$ ). With increasing density of magnetic sites the probability for an

isolated ion decreases and the zero-field heat capacity correspondingly releases continuously more entropy, before the released entropy saturates for  $x \geq 0.4$  (FIG. 1 (b)). In the half-magnetic compound the lineshape appears qualitatively similar to the dimer peak, in contrast to the anomalously broadened peak in  $\text{NaYbSe}_2$ , which reflects the geometric frustration present only in the full magnetic system. However, in all cases the release of spin entropy corresponds to a freezing of the spin degrees of freedom, and therefore in all compounds with  $x \geq 0.4$  the same proportion of spins are locked into a correlated state without long-range order.

Turning to the low-temperature behaviour, below the broad peak in  $\text{NaYbSe}_2$  the specific heat is approximately linear, with a large linear coefficient of  $\sim 1\text{ J K}^{-2}\text{ mol}^{-1}$ . This has been interpreted previously as evidence for a gapless QSL ground state [8, 16]. However, there is a significant nuclear contribution which complicates the extrapolation to zero-temperature. Further, a similar analysis applied to  $\text{NaYb}_{0.5}\text{Lu}_{0.5}\text{Se}_2$  gives a similarly large linear coefficient (as shown in FIG. 1 (d)) despite half of the magnetic sites being absent. The upturn in the half-magnetic compound is enhanced by the contribution from a small proportion of isolated ions—clearly evident at lower Yb content and perhaps arising due to a hyperfine splitting of the single ion doublet. Nevertheless the high temperature tail will also follow a  $T^{-2}$  dependence such that the fitting procedure remains valid.

The nuclear heat capacity in Yb-based systems is often primarily determined by hyperfine coupling to the unfilled  $4f$ -orbital, and fitting the nuclear contribution can therefore be used to estimate the static magnetic moment in electronic spins. This analysis requires knowledge of the electric field gradient at the Yb nucleus, which we estimate from fitting the  $\text{NaYb}_{0.05}\text{Lu}_{0.95}\text{Se}_2$  magnetisation and susceptibility data (as described in the SM alongside a description of the nuclear fitting). From this analysis we extract an average static moment of  $0.4\mu_B$  at the Yb sites in  $\text{NaYbSe}_2$ , despite there being no evidence for magnetic order at higher temperatures. Although this is far smaller than the maximum ground state moment of  $1.4\mu_B$ , it is similar in magnitude to the static moment estimated by the same method for  $\text{KYbSe}_2$  inside the magnetically ordered state [12].

Shown in FIG. 1 (e) is the zero-field longitudinal thermal conductivity across the compositional series.  $\text{NaLuSe}_2$  matches the anticipated behaviour of a non-magnetic insulator, with a single power-law  $T^{2.3}$  dependence below 500 mK. The suppression from the typical  $T^3$  phonon curve is interpreted as being due to specular scattering from the sample boundaries [20], which is feasible given that the phonon mean free path exceeds the averaged sample dimension in this temperature range (see SM). The full magnetic compound  $\text{NaYbSe}_2$  shows markedly different behaviour, with a significantly smaller magnitude thermal conductivity and a dramatic suppress-

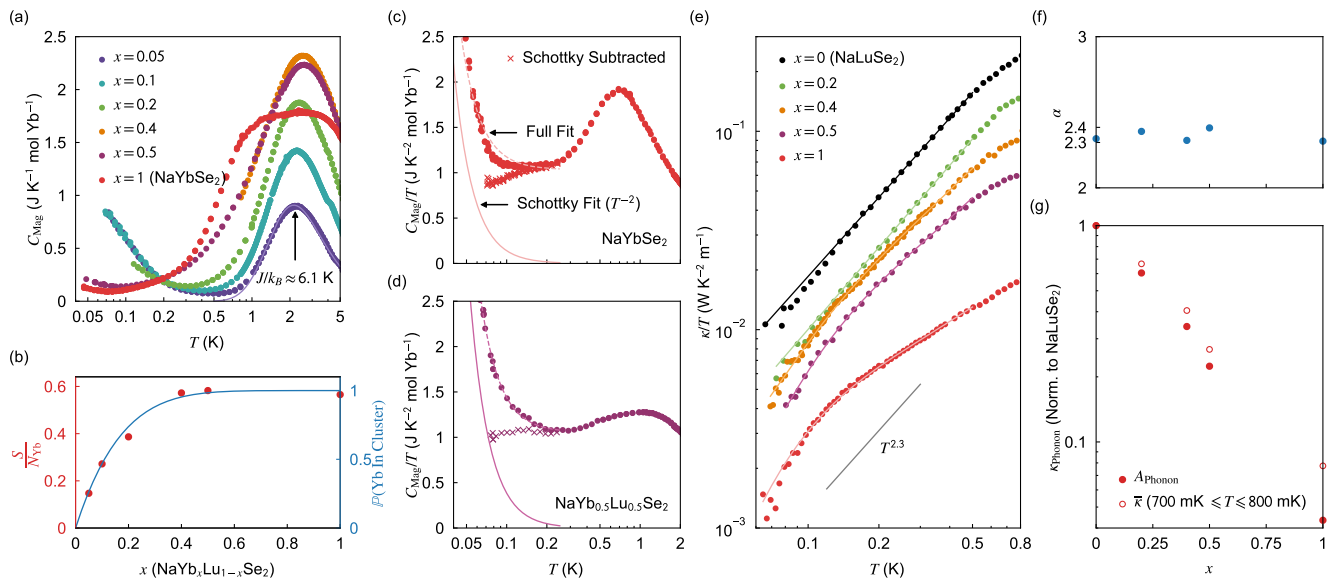


FIG. 1. (a) Zero-field magnetic heat capacity of  $\text{NaYb}_x\text{Lu}_{1-x}\text{Se}_2$ . The non-magnetic contribution has been subtracted, assuming it is identical to the  $\text{NaLuSe}_2$  heat capacity in all cases [17]. (b) The entropy release between 0.5 - 30 K, as a fraction of the anticipated entropy release according to the number of magnetic ions ( $R \ln 2$  per mole). Also included is the probability that a Yb ion will have at least one Yb nearest neighbour (see SM). (c) Low-temperature magnetic specific heat of  $\text{NaYbSe}_2$ . The dots show the measured data, the dotted line is a fit to  $aT + bT^{-2}$  and the crosses show the data with the  $bT^{-2}$  contribution (solid line) subtracted. (d) Similar for  $\text{NaYb}_{0.5}\text{Lu}_{0.5}\text{Se}_2$ . (e) Zero-field thermal conductivity of  $\text{NaYb}_x\text{Lu}_{1-x}\text{Se}_2$ . The solid lines show fits to Equation 1, as described in the main text. (f) The evolution of the phonon-term exponent  $\alpha$  as a function of Yb content  $x$ . (g) The evolution of the phonon-term coefficient  $A_{\text{Phonon}}$  and the averaged thermal conductivity between 700 - 800 mK  $\bar{\kappa}$  as a function of Yb content  $x$ .

sion at the lowest temperatures. The best fit is instead given by an exponential activation-like term plus a simple power law with exponent approximately matching the  $\text{NaLuSe}_2$  data.

Considering these end points, for temperatures below 500 mK we fit the zero-field thermal conductivity of all compounds using

$$\begin{aligned} \kappa &= \kappa_{\text{Phonon}} + \kappa_{\text{Mag}} \\ &= A_{\text{Phonon}} T^\alpha + A_{\text{Mag}} e^{-\frac{\Delta}{k_B T}}. \end{aligned} \quad (1)$$

As anticipated the lattice contribution dominates in all cases, and the fitted exponents  $\alpha$ —plotted in FIG. 1 (f)—are relatively constant throughout. Also, as shown in FIG. 1 (g), the magnitude of the thermal conductivity is exponentially suppressed with increasing proportion of magnetic sites, and this remains true across the full temperature range. Given all this, the overall suppression must be due to a broadband phonon scattering from individual magnetic sites. A strong spin-phonon coupling is natural in rare earth systems where the lowest order splitting of the spin energy levels is due to the crystalline electric field, which implies an inherent sensitivity to the ionic displacements. Indeed, previous studies have demonstrated a resonant coupling between the first crystal field excitation and the  $E_g$  phonon mode in  $\text{NaYbSe}_2$

[21, 22]. This is obviously too large an energy scale to account for the loss of thermal conductivity in this temperature regime, and instead the broadband phonon scattering might arise via single ion strain or exchange striction [23, 24].

### The Impact of Magnetic Order

Magnetic order can be induced either via the application of field or substitution of the Na site with K. A comparison against both of these cases is shown in FIG. 2. In the specific heat of  $\text{KYbSe}_2$ , the weak feature around 200 mK is interpreted as evidence for the onset of magnetic order. This contrasts with the sharp transition observed in a previous study [12], but matches a similarly weak feature observed in the heat capacity at the ordering transition in  $\text{CsYbSe}_2$  [11]. This is perhaps related to sample quality, but regardless in all cases the vast majority of entropy is released above the transition to long-range order, suggesting that only a small proportion of the spin degrees of freedom order at this temperature.

Also included in FIG. 2 is the measured thermal conductivity in each of these cases. As mentioned, for  $\text{NaYbSe}_2$  in zero-field this follows a behaviour similar to  $\kappa_{\text{Mag}} \sim e^{-\frac{\Delta}{k_B T}}$ , which implies an energy gap  $\Delta$  in

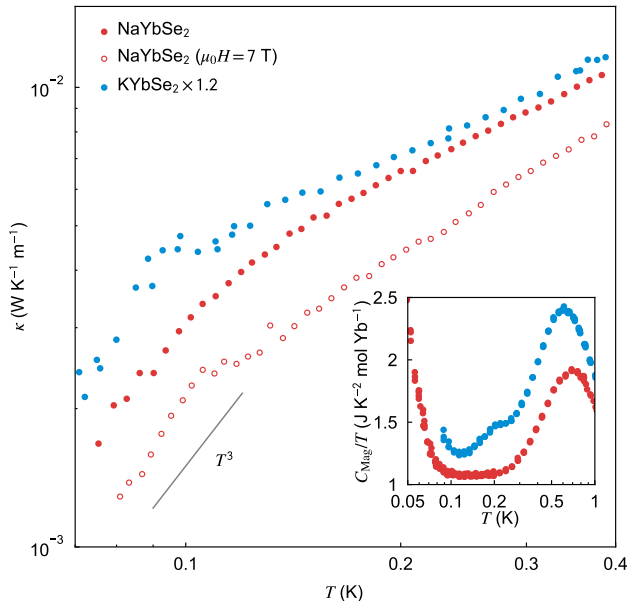


FIG. 2. Thermal conductivity of NaYbSe<sub>2</sub> and KYbSe<sub>2</sub> in zero-field, and of NaYbSe<sub>2</sub> in a field of 7 T. The inset shows the low-temperature magnetic heat capacity for the zero-field measurements. See SM for the in-field data, wherein the nuclear contribution is strongly enhanced and obscures any evidence for a transition.

the dispersion spectrum of the corresponding magnetic itinerant energy carrier. In stark contrast, distinct sharp kinks are observed in the thermal conductivity of KYbSe<sub>2</sub> or in NaYbSe<sub>2</sub> under field, below which the data follows an approximate  $T^3$  power law. This matches the expectation for antiferromagnetic magnons, and the sharp kinks therefore signal the anticipated transition to long-range magnetic order.

Near and above the transition at  $T_N$ , non-coherent thermal fluctuations in magnetic spin textures dominate over the nearest-neighbour spin-spin interactions. The heat capacity of these critical fluctuations should roughly follow  $1/(T - T_N)^{2\nu}$  (discussed in the SM), which translates to a shoulder-like feature in the thermal conductivity. The absence of a similar kink-like feature in the zero-field thermal conductivity of NaYbSe<sub>2</sub> substantiates the claim that there is no long-range order down to 60 mK. Further, we can now confidently rule out AFM magnons or near-critical thermal fluctuations—both induced by long-range AFM order—in the interpretation of the exponential downturn.

### Comparisons Across the Percolation Transition

We can further investigate the nature of the magnetic excitations in the disordered phase of NaYbSe<sub>2</sub> by

tracking their evolution across the compositional series. The unique self-duality between occupied and unoccupied sites on the two-dimensional triangular lattice puts the site percolation threshold at exactly  $x_C = 0.5$ . Only above this threshold do there exist connected magnetic components of a size comparable to that of the entire lattice. However, while the percolation threshold is sharp in its mathematical definition the physical reality might not be so clear cut. For example, in thermal transport the flow of entropy between disconnected magnetic clusters is facilitated by the aforementioned spin-phonon coupling. This is presumably why the data of the 40% and 50% compounds appears similar, and we therefore only include the latter in this discussion.

A comparison of lattice configuration, specific heat and thermal conductivity for select compositions is shown in FIG. 3. For NaYb<sub>0.2</sub>Lu<sub>0.8</sub>Se<sub>2</sub>, as illustrated in the left panels of the plot, the Yb<sup>3+</sup> clusters are small and well isolated from one another. The magnetic specific heat appears similar to the isolated dimer singlet condensation peak in NaYb<sub>0.05</sub>Lu<sub>0.95</sub>Se<sub>2</sub>, and can also be attributed to the entropy release from small isolated clusters as they each fall into their respective ground state. This picture of isolated clusters is supported by the thermal conductivity, wherein we observe the exact same phonon behaviour as in the non-magnetic NaLuSe<sub>2</sub>, albeit with a reduced overall magnitude due to phonon scattering by the small proportion of spins present.

Jumping to NaYb<sub>0.5</sub>Lu<sub>0.5</sub>Se<sub>2</sub>—shown in the middle panels of FIG. 3, and which sits at the percolation threshold—the majority of magnetic clusters are now connected. The specific heat features a single peak that is enhanced and broadened from the peak of NaYb<sub>0.2</sub>Lu<sub>0.8</sub>Se<sub>2</sub>, as a result of the increased number of both magnetic ions and configurations of magnetic cluster. However, the qualitative similarity reflects the absence of any significant geometric frustration in either compound—regardless of size all magnetic clusters are free to relax into their respective ground states, and this occurs at approximately the energy scale of exchange. In the magnetic thermal conductivity we observe a broad downturn below 500 mK. In this temperature range the data is well fit using the generic gap function given in Equation 1, yielding a gap  $\Delta/k_B \approx 441$  mK.

Finally, in NaYbSe<sub>2</sub> (shown in the right panels of FIG. 3) the full two-dimensional triangular AFM lattice confers strong geometric frustration on all sites. Above 500 mK this manifests as a plateau-like feature in the specific heat as the spin moments struggle to release entropy. This contrasts with NaYb<sub>0.5</sub>Lu<sub>0.5</sub>Se<sub>2</sub> (and indeed all compounds with  $x \leq 0.5$ ), but it is worth re-iterating that in both cases the same proportion of spin entropy is released above 500 mK. In the magnetic thermal conductivity, despite the magnitude being approximately half that of NaYb<sub>0.5</sub>Lu<sub>0.5</sub>Se<sub>2</sub>, there is no qualitative difference and the data can be fit to the same gap function.

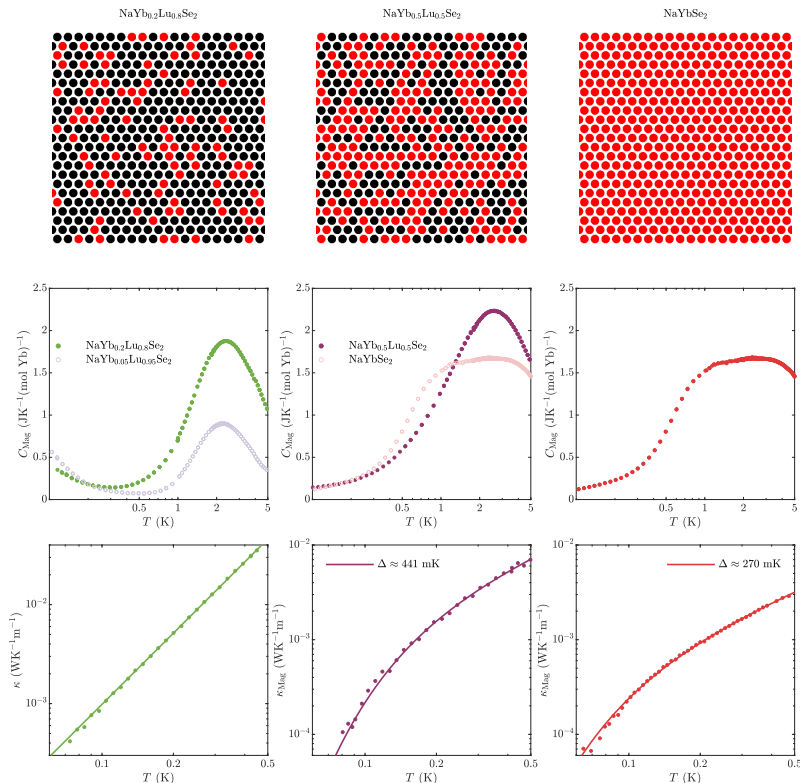


FIG. 3. Detailed comparison across the compositional series. The top panels show a schematic random distribution of magnetic (red,  $\text{Yb}^{3+}$ ) and non-magnetic (black,  $\text{Lu}^{3+}$ ) sites, the middle panels show the magnetic specific heat, and the bottom panels show the thermal conductivity. The  $\text{NaYb}_{0.2}\text{Lu}_{0.8}\text{Se}_2$  also includes the fit to a single power law. For  $\text{NaYb}_{0.5}\text{Lu}_{0.5}\text{Se}_2$  and  $\text{NaYbSe}_2$  the phonon contribution has been subtracted, and the fits to the magnetic thermal conductivity are from Equation 2.

This gives a slightly smaller but comparable spectral gap of  $\Delta/k_B \approx 270$  mK.

## DISCUSSION

Interest in  $\text{NaYbSe}_2$  stems from its candidacy as a QSL material, and we begin by exploring our observations within that context. The large linear coefficient in the low-temperature specific heat points towards there being some gapless excitation, whereas the thermal conductivity shows definitively gapped behaviour—this opens the door to diametrically opposed interpretations. Pertinently, the well-established triangular lattice QSL candidate  $\kappa$ -(BEDT-TTF) $_2\text{Cu}_2(\text{CN})_3$  also exhibits this same conflict of experimental findings [25, 26]. In this case, one interpretation is that the downturn in the thermal conductivity might be due to an inhomogeneity-induced localisation of gapless spinon excitations [27], whereas another is that the linear coefficient in the specific heat might be an artefact arising due to an incorrect estimation of the nuclear contribution [28], such that the QSL ground state is gapped. Similar dichotomies also exist in other notable QSL candidates—for example the closely

related compound  $\text{YbMgGaO}_4$  [29–31] or the honeycomb lattice compound  $\text{Na}_2\text{Co}_2\text{TeO}_6$  [32, 33]—suggesting that this might be an intrinsic universal feature rather than an experimental disagreement. However, all compounds suffer from some form of disorder, and all have been accused of QSL mimicry as a result [14, 15, 34]. For  $\text{NaYbSe}_2$  studied in isolation, all these interpretations remain valid. The most we can say with certainty is that if there do exist gapless excitations then they cannot be good thermal carriers.

However, this study leverages site dilution as a novel means for comparison, and as such we are able to move beyond a mapping onto some poorly defined QSL ground state. The most crucial aspect of this approach is that above some threshold of site dilution the relevant length scales and connectivity will be determined by a known concentration of randomly distributed non-magnetic sites, rather than an unknown degree of random disorder.  $\text{NaYb}_{0.5}\text{Lu}_{0.5}\text{Se}_2$  is certainly within the former regime, and we can therefore draw comparisons with the full magnetic compound in order to better understand the low-energy excitations.

In  $\text{NaYb}_{0.5}\text{Lu}_{0.5}\text{Se}_2$ , given the long-range connectivity but small degree of frustration, the magnetic lattice

might be considered as a collection of interwoven one-dimensional spin chains and ladders. This motivates us to fit the thermal conductivity using

$$\kappa_{\text{Mag}} = A_{\text{Mag}} T \int_{\Delta/(k_B T)}^{x_{\text{max}}} \frac{x^2 e^x}{(e^x - 1)^2} dx, \quad (2)$$

which is simply the thermal conductivity of a one-dimensional bosonic carrier with a gapped linear dispersion. In this expression,  $\Delta$  is the spectral gap of the corresponding itinerant magnetic energy carrier, while  $x_{\text{max}} = \epsilon_{\text{max}}/(k_B T)$  reflects the maximum energy  $\epsilon_{\text{max}}$  of said carrier [35]. This modeling is discussed more thoroughly in the SM, and a fit to the magnetic thermal conductivity of  $\text{NaYb}_{0.5}\text{Lu}_{0.5}\text{Se}_2$  is included in FIG. 3. In those materials which do consist of one-dimensional spin chains, the presence of a gap is typically understood as arising due to local anisotropy. In this case the gap is harder to interpret, but perhaps might arise from small amounts of remnant frustration. Regardless of the origin however, due to the random nature of the magnetic lattice the fitted gap energy will be an effective averaging over all contributions and spatial inhomogeneities.

Also included in FIG. 3 is the same fitting for  $\text{NaYbSe}_2$ , which demonstrates that the same model can still adequately describe the data.  $\text{NaYbSe}_2$  is obviously far removed from a system of isolated one-dimensional spin chains, but the concept of inhomogeneity might still be relevant. Specifically, we believe the existence of short-range ordered regions has strong support from three key, existing pieces of evidence: (i) a near-unitary majority of the electronic spin entropy being released above 500 mK, implying that the vast majority of spins will be confined (or close) to the ground state below this temperature, (ii) the non-zero static moment of  $0.4\mu_B$  measured through fitting the nuclear specific heat, indicating a non-vanishing amount of spin ordering, and (iii) the appearance of intensity peaks consistent with  $120^\circ$  order, as measured by inelastic neutron scattering [16]. Moreover, (i), (ii) and (iii) are similarly true for  $\text{KYbSe}_2$ , which clearly does order [12]. Crucially, in the magnetically ordered phase of  $\text{CsYbSe}_2$  the in-plane spin correlation length was estimated to be only  $60 \text{ \AA}$ , and the ordered moment only  $0.1\mu_B$  (a small fraction of the full ground state moment) [11]. One could envisage a situation where the in-plane correlation length shrinks with increasing next-nearest neighbour interaction strength—similar to the AFM transition temperature—but remains finite in  $\text{NaYbSe}_2$ . The dominant magnetic thermal pathways might then occur at the boundaries of short-range ordered regions, analogous to the situation in  $\text{NaYb}_{0.5}\text{Lu}_{0.5}\text{Se}_2$  where the magnetic thermal carriers are forced to travel along the percolation pathways.

This proposal would explain the lack of long-range ordering measured by any bulk probe, but also the low-temperature peaks consistent with  $120^\circ$  short-range order observed via inelastic neutron scattering [16]. With

decreasing temperature these short-range ordered regions will either coalesce at a transition to long-range order or be prevented from doing so by quenched disorder and instead freeze into a spin glass state. According to some proposals, this second option might be the ultimate fate of any geometrically frustrated system which avoids long-range order [36]. Indeed, in the closely related compounds  $\text{YbZnGaO}_4$  and  $\text{YbMgGaO}_4$  a downturn in the thermal conductivity—with corresponding extrapolated negative  $\kappa/T$  at zero-temperature—is observed as a precursor to the spin glass transition, which manifests as a drop in the measured AC magnetic susceptibility at a slightly lower temperature [37].

Through low-temperature thermal conductivity measurements we have demonstrated the presence of a gapped magnetic excitation in  $\text{NaYbSe}_2$ . Through comparisons against magnetically ordered  $\text{KYbSe}_2$  and  $\text{NaYbSe}_2$  in field, and across the compositional series  $\text{NaYb}_x\text{Lu}_{1-x}\text{Se}_2$ , we have strong evidence that this excitation is not from the quantum spin liquid ground state. The similarity between  $\text{NaYbSe}_2$  and  $\text{NaYb}_{0.5}\text{Lu}_{0.5}\text{Se}_2$  implies that the gapped excitation does not emerge from a heightened geometric frustration, and instead that inhomogeneity should be more relevant. This leads us to conclude that there exist short-range ordered regions in  $\text{NaYbSe}_2$ , separated by entropy-carrying boundaries. The apparent ubiquity of a downturn in the thermal conductivity of spin liquid candidates further suggests that this concept might be relevant to a whole host of materials, regardless of composition or even magnetic structure.

This work was supported by the U.S. Department of Energy, Office of Science, Basic Energy Sciences, Materials Sciences and Engineering Division under contract DE-AC02-05-CH11231 within the Quantum Materials program (KC2202). J.G.A., L.P.C. and Y.L. were supported by the EPiQS Initiative of the Gordon and Betty Moore Foundation through grant no. GBMF9067. C.L. acknowledges the fellowship support from the Gordon and Betty Moore Foundation through the Emergent Phenomena in Quantum Systems (EPiQS) program. Work at the National High Magnetic Field Laboratory was supported by NSF Cooperative Agreements No. DMR-1644779 and No. DMR-2128556, the U.S. Department of Energy (DOE), and the State of Florida. J.S. acknowledges support from the DOE Basic Energy Sciences FWP “Science of 100 T”.

---

\* Equal contribution; Email: lpc@berkeley.edu

† Equal contribution

‡ Corresponding author; Email: analytis@berkeley.edu

- [1] D. A. Huse and V. Elser, *Phys. Rev. Lett.* **60**, 2531 (1988).  
 [2] Z. Zhu and S. R. White, *Phys. Rev. B* **92**, 41105 (2015).  
 [3] J. Iaconis, C. Liu, G. B. Halász, and L. Balents, *SciPost*

- Phys. **4**, 3 (2018).
- [4] W.-J. Hu, S.-S. Gong, W. Zhu, and D. N. Sheng, Phys. Rev. B **92**, 140403 (2015).
- [5] Y. Iqbal, W.-J. Hu, R. Thomale, D. Poilblanc, and F. Becca, Phys. Rev. B **93**, 144411 (2016).
- [6] D.-V. Bauer and J. O. Fjærestad, Phys. Rev. B **96**, 165141 (2017).
- [7] S. Hu, W. Zhu, S. Eggert, and Y.-C. He, Phys. Rev. Lett. **123**, 207203 (2019).
- [8] K. M. Ranjith, S. Luther, T. Reimann, B. Schmidt, P. Schlender, J. Sichelschmidt, H. Yasuoka, A. M. Strydom, Y. Skourski, J. Wosnitza, H. Kühne, T. Doert, and M. Baenitz, Phys. Rev. B **100**, 224417 (2019).
- [9] J. Xing, L. D. Sanjeeva, J. Kim, G. R. Stewart, A. Podlesnyak, and A. S. Sefat, Phys. Rev. B **100**, 220407 (2019).
- [10] J. Xing, L. D. Sanjeeva, A. F. May, and A. S. Sefat, APL Materials **9**, 111104 (2021).
- [11] T. Xie, A. A. Eberharter, J. Xing, S. Nishimoto, M. Brando, P. Khanenko, J. Sichelschmidt, A. A. Turriani, D. G. Mazzone, P. G. Naumov, L. D. Sanjeeva, N. Harrison, A. S. Sefat, B. Normand, A. M. Läuchli, A. Podlesnyak, and S. E. Nikitin, npj Quantum Materials **8**, 48 (2023).
- [12] A. O. Scheie, E. A. Ghioldi, J. Xing, J. A. M. Paddison, N. E. Sherman, M. Dupont, L. D. Sanjeeva, S. Lee, A. J. Woods, D. Abernathy, D. M. Pajerowski, T. J. Williams, S.-S. Zhang, L. O. Manuel, A. E. Trumper, C. D. Pemmaraju, A. S. Sefat, D. S. Parker, T. P. Devereaux, R. Movshovich, J. E. Moore, C. D. Batista, and D. A. Tennant, Nature Physics **20**, 74 (2024).
- [13] R. S. Dissanayaka Mudiyansele, H. Wang, O. Vilella, M. Mourigal, G. Kotliar, and W. Xie, Journal of the American Chemical Society **144**, 11933 (2022).
- [14] Z. Zhu, P. A. Maksimov, S. R. White, and A. L. Chernyshev, Phys. Rev. Lett. **119**, 157201 (2017).
- [15] A. Pustogow, Solids **3**, 93 (2022).
- [16] P.-L. Dai, G. Zhang, Y. Xie, C. Duan, Y. Gao, Z. Zhu, E. Feng, Z. Tao, C.-L. Huang, H. Cao, A. Podlesnyak, G. E. Granroth, M. S. Everett, J. C. Neufeind, D. Voneshen, S. Wang, G. Tan, E. Morosan, X. Wang, H.-Q. Lin, L. Shu, G. Chen, Y. Guo, X. Lu, and P. Dai, Phys. Rev. X **11**, 21044 (2021).
- [17] L. Pritchard Cairns, R. Day, S. Haley, N. Maksimovic, J. Rodriguez, H. Taghinejad, J. Singleton, and J. Analytis, Phys. Rev. B **106**, 24404 (2022).
- [18] R. Bachmann, F. J. DiSalvo, T. H. Geballe, R. L. Greene, R. E. Howard, C. N. King, H. C. Kirsch, K. N. Lee, R. E. Schwall, H. Thomas, and R. B. Zubeck, Rev. Sci. Instrum. **43**, 205 (1972).
- [19] J. S. Hwang, K. J. Lin, and C. Tien, Review of Scientific Instruments **68**, 94 (1997).
- [20] S. Y. Li, J.-B. Bonnemaïson, A. Payeur, P. Fournier, C. H. Wang, X. H. Chen, and L. Taillefer, Phys. Rev. B **77**, 134501 (2008).
- [21] Z. Zhang, X. Ma, J. Li, G. Wang, D. T. Adroja, T. P. Perring, W. Liu, F. Jin, J. Ji, Y. Wang, Y. Kamiya, X. Wang, J. Ma, and Q. Zhang, Phys. Rev. B **103**, 35144 (2021).
- [22] Y.-Y. Pai, C. E. Marvinney, G. Pokharel, J. Xing, H. Li, X. Li, M. Chilcote, M. Brahlek, L. Lindsay, H. Miao, A. S. Sefat, D. Parker, S. D. Wilson, J. S. Gardner, L. Liang, and B. J. Lawrie, Advanced Science **11**, 2304698 (2024).
- [23] B. Lüthi, *Physical Acoustics in the Solid State* (Springer Science and Business Media, 2007).
- [24] S. Erfanifam, S. Zherlitsyn, S. Yasin, Y. Skourski, J. Wosnitza, A. A. Zvyagin, P. McClarty, R. Moessner, G. Balakrishnan, and O. A. Petrenko, Phys. Rev. B **90**, 64409 (2014).
- [25] S. Yamashita, Y. Nakazawa, M. Oguni, Y. Oshima, H. Nojiri, Y. Shimizu, K. Miyagawa, and K. Kanoda, Nature Physics **4**, 459 (2008).
- [26] M. Yamashita, N. Nakata, Y. Kasahara, T. Sasaki, N. Yoneyama, N. Kobayashi, S. Fujimoto, T. Shibauchi, and Y. Matsuda, Nature Physics **5**, 44 (2009).
- [27] S. Yamashita, T. Yamamoto, Y. Nakazawa, M. Tamura, and R. Kato, Nature Communications **2**, 275 (2011).
- [28] A. P. Ramirez, Nature Physics **4**, 442 (2008).
- [29] Y. Li, H. Liao, Z. Zhang, S. Li, F. Jin, L. Ling, L. Zhang, Y. Zou, L. Pi, Z. Yang, J. Wang, Z. Wu, and Q. Zhang, Scientific Reports **5**, 16419 (2015).
- [30] Y. Xu, J. Zhang, Y. S. Li, Y. J. Yu, X. C. Hong, Q. M. Zhang, and S. Y. Li, Phys. Rev. Lett. **117**, 267202 (2016).
- [31] X. Rao, G. Hussain, Q. Huang, W. J. Chu, N. Li, X. Zhao, Z. Dun, E. S. Choi, T. Asaba, L. Chen, L. Li, X. Y. Yue, N. N. Wang, J.-G. Cheng, Y. H. Gao, Y. Shen, J. Zhao, G. Chen, H. D. Zhou, and X. F. Sun, Nature Communications **12**, 4949 (2021).
- [32] G. Lin, J. Jeong, C. Kim, Y. Wang, Q. Huang, T. Masuda, S. Asai, S. Itoh, G. Günther, M. Russina, Z. Lu, J. Sheng, L. Wang, J. Wang, G. Wang, Q. Ren, C. Xi, W. Tong, L. Ling, Z. Liu, L. Wu, J. Mei, Z. Qu, H. Zhou, X. Wang, J.-G. Park, Y. Wan, and J. Ma, Nature Communications **12**, 5559 (2021).
- [33] X. Hong, M. Gillig, W. Yao, L. Janssen, V. Kocsis, S. Gass, Y. Li, A. U. B. Wolter, B. Büchner, and C. Hess, npj Quantum Materials **9**, 18 (2024).
- [34] L. Xiang, R. Dhakal, M. Ozerov, Y. Jiang, B. S. Mou, A. Ozarowski, Q. Huang, H. Zhou, J. Fang, S. M. Winter, Z. Jiang, and D. Smirnov, Phys. Rev. Lett. **131**, 76701 (2023).
- [35] A. V. Sologubenko, K. Gianno, H. R. Ott, U. Ammerahl, and A. Revcolevschi, Phys. Rev. Lett. **84**, 2714 (2000).
- [36] S. V. Syzranov and A. P. Ramirez, Nature Communications **13**, 2993 (2022).
- [37] Z. Ma, J. Wang, Z.-Y. Dong, J. Zhang, S. Li, S.-H. Zheng, Y. Yu, W. Wang, L. Che, K. Ran, S. Bao, Z. Cai, P. Cermak, A. Schneidewind, S. Yano, J. S. Gardner, X. Lu, S.-L. Yu, J.-M. Liu, S. Li, J.-X. Li, and J. Wen, Phys. Rev. Lett. **120**, 87201 (2018).